Published in final edited form as:

*Int J Pharm*. 2020 January 05; 573: 118894. doi:10.1016/j.ijpharm.2019.118894.

# Efficient Inhibition of Uveal Melanoma via Ternary siRNA Complexes

**Lingxiao Xie**[a], **Yan Yang**[a,b], **Jie Shen**[a,c,*]

[a]Department of Biomedical and Pharmaceutical Sciences, University of Rhode Island, Kingston, RI, 02881, USA

[b]College of Pharmaceutical Science, Zhejiang University of Technology, Hangzhou, 310014, China

[c]Department of Chemical Engineering, University of Rhode Island, Kingston, RI, 02881, USA

## Abstract

Uveal melanoma (UM) is rare yet the most common and malignant primary intraocular tumor in adults. Due to the lack of effective treatment, the mortality rate of UM has remained high over the past few decades. In the present study, hyaluronic acid (HA) coated chitosan (Chi)/siRNA ternary complexes have been developed and characterized as a novel therapeutic strategy molecularly targeting hypoxia-inducible factor 1α (HIF-1α) pathway for the treatment of UM. The cytotoxicity, cellular uptake, and siRNA silencing effect of the developed siRNA complexes were evaluated. In addition, whether the developed ternary complexes can inhibit UM migration and invasion was investigated. Results showed that the developed ternary siRNA complexes were negatively charged and with a particle size below 190 nm. The ternary siRNA complexes showed excellent cellular uptake and lysosome escape ability with low cytotoxicity. In addition, the ternary complexes were able to downregulate both HIF-1α and VEGF expression in UM cells, and successfully inhibit UM migration and invasion. These results demonstrated that the biocompatible ternary siRNA complexes are promising for local treatment of UM in the posterior segment with future clinical application potential.

## Graphical Abstract

*Address for Correspondence: Jie Shen, Departments of Biomedical and Pharmaceutical Sciences and Chemical Engineering, University of Rhode Island, 7 Greenhouse Road, Kingston, RI 02881, USA, jie_shen@uri.edu, Telephone: 401-874-5594.



Declaration of interests

The authors declare that they have no known competing financial interests or personal relationships that could have appeared to influence the work reported in this paper.

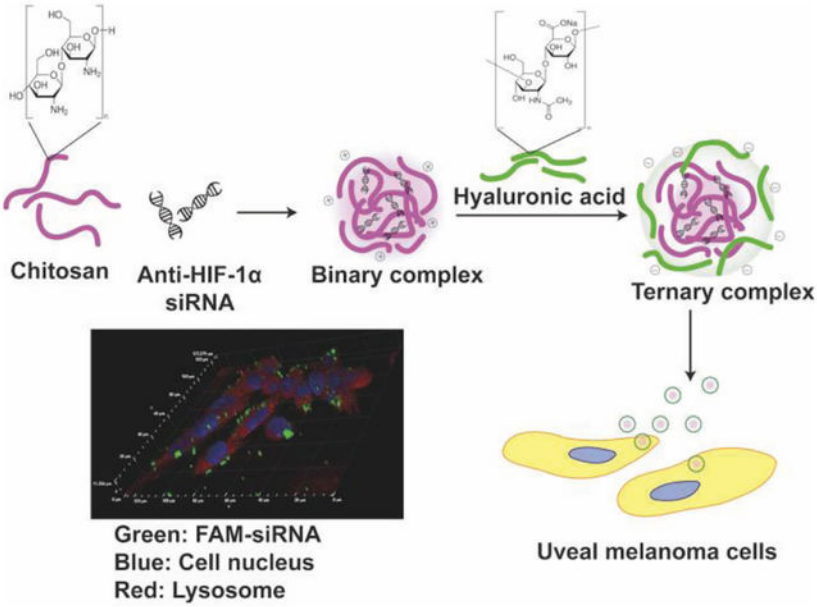


**Keywords**

uveal melanoma; hypoxia-inducible factor 1α (HIF-1α); hyaluronic acid; ternary siRNA complex; metastasis

## 1. INTRODUCTION

Uveal melanoma (UM) is rare yet the most common primary intraocular tumor in adult, accounting for 5% of all melanomas and 13% of melanoma deaths (Harbour, 2012; Kaliki and Shields, 2016). At present, the common first-line treatments for this malignancy include eye enucleation, radiation (e.g. brachytherapy), and surgical resection. However, aggressive treatment such as enucleation and irradiation is not an “immediate treatment” option when tumor is below 16 mm in diameter and 9 mm in thickness (Shields et al., 2009). Nearly half of UM patients ultimately develop distant metastases (predominantly to the liver) that are notoriously resistant to systemic chemo- and immunotherapy, with a median survival of five to seven months after the detection of metastasis (Bhatia et al., 2012; Damato, 2006; Diener-West et al., 1992; Moser et al., 2015; Spagnolo et al., 2012). Despite advances in the diagnosis and localized treatment over the past decades, there is currently no effective therapies for the treatment of UM (Munzenrider, 2001).

Posterior UM (e.g. choroidal and ciliary body) accounting for more than 95% of UM cases, exhibit a strong tendency for lethal liver metastasis, thus poor prognosis and high mortality (Carvajal et al., 2017; Woodman, 2012). The uvea is one of the most capillary-rich tissues of the body, yet lack of lymphatic drainage. Therefore, UM metastatic spread occurs strictly via the hematogenous route (Amirouchene-Angelozzi et al., 2015; Onken et al., 2014). Metastasis is a major challenge not only in UM therapy, but also in overall clinical management of many cancers. It is considered that metastasis involves critical interactions between tumor cells and microenvironment. For instance, hypoxia environment promotes

metastatic progression of cancer cells. Clinically, overexpression of hypoxia-inducible transcription factors in various cancer types is associated with increased distant metastasis and poor survival (Rankin and Giaccia, 2016). Downregulation of hypoxia-inducible factor (HIF) has been shown to decrease metastatic potential of various tumor cells such as breast cancer, lung cancer, and melanoma (Hanna et al., 2013; Hiraga et al., 2007; Liao et al., 2007; Wong et al., 2011; Zhang et al., 2012). HIF-1α, a transcription factor regulates the expression of secreted factors that mediate angiogenesis and tumor metastasis, is strongly associated with the gene expression profile of Class 2 UM (very likely to metastasize) (Asnaghi et al., 2014; Hu et al., 2016; Martinengo et al., 2014; Mouriaux et al., 2014). Although downregulating HIF-1α via either lentivirus-mediated short hairpin RNA (shRNA) delivery or a small molecule HIF-1α inhibitor digoxin showed inhibition of UM cell invasion *in vitro* (Asnaghi et al., 2014), these therapeutic strategies are not practical for localized treatment against UM metastasis in the posterior segment due to their intrinsic toxicity and side effects.

In the present study, a novel, biocompatible ternary siRNA complex was developed to deliver molecularly targeted anti-HIF-1α siRNA in the posterior eye segment to inhibit UM progression and invasion via downregulating HIF-1α gene expression in UM cells. Chitosan is one of the most commonly used polycations in gene delivery due to its relatively low toxicity, low immunogenicity, and high biocompatibility (Gao et al., 2005; Ghosh et al., 2007; Mansouri et al., 2004; Mao et al., 2010). However, high positive charge density in high molecular weight (MW) chitosan can lead to slow siRNA release due to strong electrostatic interaction, resulting in delayed or impaired gene silencing effect (MacLaughlin et al., 1998; Mao et al., 2010). Moreover, high MW chitosan is often associated with poor water solubility under physiological environment, which may hamper its complexion ability with siRNA (Dehousse et al., 2010). Accordingly, a water-soluble, low MW chitosan oligosaccharide lactate (Chi) has been selected as a carrier to condense anti-HIF-1α siRNA to form Chi/siRNA nanocomplexes. In order to avoid immobilization of the nanocomplexes in the vitreous humor and facilitate their transport to the tumor site (Martens et al., 2015; Xu et al., 2013). An anionic coating of hyaluronic acid (HA), a non-immunogenic and ubiquitous biopolymer in human organisms including vitreous humor, was used to shield the cationic charge of the Chi/siRNA nanocomplexes and facilitate transport of the nanocomplexes in the vitreous humor (Martens et al., 2015; Xu et al., 2013). The therapeutic strategy via ternary Chi/siRNA nanocomplexes for the treatment of UM was assessed.

## 2. METHODS

### 2.1. Materials and cell culture

Chitosan oligosaccharide lactate (Chi, MW: 5 kDa), formaldehyde solution (molecular biology), Transwell® insert (6.5 mm insert, 8.0 μm polycarbonate membrane, Corning®), 0.45 μm Immobilion®-P PVDF transfer membrane, and sodium dodecyl sulfate (SDS) were purchased from Millipore Sigma (St. Louis, MO). Sodium hyaluronate (HA, MW: 20 kDa) was purchased from Lifecore Biomedical (Chaska, MN). UranyLess EM stain was purchased from Electron Microscopy Sciences (Hatfield, PA). Water (diethylpyrocarbonate (DEPC)-treated, DNase- and RNase-free, Fisher BioReagents™), and IBI scientific 3P 6X

gel loading dye were purchased from Fisher Scientific (Hampton, NH). MTT Cell Proliferation Assay Kit (Vybrant™), SuperScript™ IV First-Strand Synthesis System (Invitrogen™), TRIzol™ Reagent, glyceraldehyde 3-phosphate dehydrogenase (GAPDH, # Hs02786624_g1), TaqMan™Gene Expression Assay (FAM), HIF-1α (# Hs00153153_m1), M-PER™ Mammalian Protein Extraction Reagent, Halt™ Protease Inhibitor Cocktails, Pierce™ BCA Protein Assay Kit, HIF-1α monoclonal antibody (mgc3), SuperSignal™ West Pico PLUS Chemiluminescent substrate protocol, Corning® Matrigel® Matrix (growth factor reduced), Trypsin-EDTA (0.25%), 1% Penicillin-Streptomycin, Lyso Tracker Red DND-99 (Invitrogen™), Hoechst (Invitrogen™), and phosphate buffered saline (PBS, pH 7.2) were purchased from Thermo Fisher Scientific (Waltham, MA). 4–20% Mini-PROTEAN® TGX™ Precast Gel and 4x Laemmli Sample Buffer were purchased from Bio-Rad (Hercules, CA). GAPDH (6C5) and C were purchased from Santa Cruz biotechnology (Dallas, TX). Anti-mouse IgG, HRP-linked antibody and nuclease-free water were purchased from Cell Signaling Technology (Danvers, MA). Fetal bovine serum (FBS), Dulbecco's PBS (D-PBS, 1X), Dulbecco's Modified Eagle's Medium (DMEM), and RPMI-1640 medium were purchased from ATCC (The Global Bioresource Center, Manassas, VA).

siRNA targeting HIF-1α (siGENOME Human HIF-1α siRNA, target sequence *GAYGAAAGAAYYACCGAAU*), scramble siRNA (siGENOME Non-Targeting siRNA, target sequence *AUGAACGUGAAUUGCUCAA*), FAM-siRNA (siGLO Green 6-FAM), and DharmaFECT1 (DF) transfection reagents were purchased from Dharmacon (Lafayette, CO).

Human UM cell line MP-38 (ATCC CRL-3296) was grown and maintained in RPMI-1640 media with 20% FBS and 1% Penicillin-Streptomycin. NIH3T3 cell line was kindly provided by Dr. Roxbury (University of Rhode Island) and maintained in DMEM media with 10% FBS and 1% Penicillin-Streptomycin. The cells were cultured in an incubator supplied with 5% $CO_2$ at 37°C. The culture medium was changed every 2–3 days. For hypoxic conditions, the cells were incubated in an atmosphere of 1% $O_2$, 5% $CO_2$, and 94% $N_2$ in a hypoxia incubator chamber (STEMCELL™ Technologies) based on the product protocol.

### 2.2. Preparation of Chi/siRNA complexes

The complex fabrication process was performed in the neutral environment without the use of any acidic buffer and organic solvents. Briefly, solutions of Chi (10 μM), HIF-1α siRNA (0.5 μM), and HA (50 μM) were prepared in DEPC-treated water separately. Different molar ratios of the Chi and siRNA solutions were mixed and incubated for 30 min at room temperature to form binary Chi/siRNA complexes. For ternary complexes, a given volume of HA solution was added to the binary Chi/siRNA complexes, and the mixture was then incubated for another 30 min at room temperature. Different HA/Chi/siRNA (C/N/P) molar ratios were investigated.

### 2.3. Characterization of Chi/siRNA complexes

The hydrodynamic diameter ($D_H$, Z-average size), polydispersity index (PDI) and zeta potential (ξ) of the prepared siRNA complexes were measured using Zetasizer Nano ZS90 (Malvern Instruments Ltd., Malvern, UK). The backscattering angel was 173° with a standard laser wavelength λ of 633 nm. The measurement of $D_H$ is according to the Stokes-Einstein equation as a function of the diffusion coefficient (D), temperature (T), and viscosity (η).

The siRNA loading efficiency was determined using agarose gel electrophoresis. Naked siRNA (0.25 μM) was studied as a control. siRNA complexes with different C/N/P molar ratios and the naked siRNA were gently mixed with 6X gel loading dye and applied onto an agarose gel (1.2%, w/v) with ethidium bromide to stain siRNA. The electrophoresis was carried out at a voltage of 100 V for 45 min in Tris-acetate-EDTA (TAE) buffer. The loading efficiency was calculated based on the equation (1) below:

$$siRNA\ Loading\ Efficiencey(\%) = (1 - \frac{free\ siRNA}{siRNA\ loading\ amount}) \times 100\% \quad (1)$$

Morphology of the complexes was studied using transmission electron microscopy (TEM, JEM 2100, JEOL Ltd, Japan) bright field. 5 μL of complex suspensions were deposited on copper grids. The grids were then dried in air for 1 hr at room temperature followed by staining with UranyLess stain to enable polymer visualization. The stained samples were dried in air for 1 hr before TEM imaging.

### 2.4. Stability evaluation of Chi/siRNA complexes

The stability of the developed siRNA complexes was evaluated using gel electrophoresis. The complexes with different C/N/P ratio were incubated with ribonuclease A (RNase A) (0.01 U/μg siRNA) at 37°C for different duration. After the incubation, the complexes were disassociated by 2% SDS. All samples were run in electrophoresis gel at 100 mV for 45 min.

### 2.5. Cytotoxicity assay

The cytotoxicity of the Chi/siRNA complexes with and without HA coating in MP-38 cells was investigated by measuring their metabolic activity via a MTT assay under hypoxia conditions. Polymer solutions studied as controls included: Chi solutions at the same concentrations as that used in the complexes at N/P molar ratios of 20/1 (low conc.) and 40/1 (high conc.); HA solutions at the same concentrations as that used in the ternary siRNA complexes at C/P molar ratios of 10/1 (low conc.) and 40/1 (high conc.); and a commercial transfection reagent (DF). MP-38 cells were seeded in a 96-well plate with a density of $2\times10^4$ cells per well and incubated till the confluency reached about 80%. Prior to the complex treatment, the culture medium was removed and the cells were washed with PBS buffer, and the serum free medium was added to the wells. 20 μL of the complexes with various C/N/P molar ratios but the same siRNA amount (67 nM) were added into each well. After a 24-hr treatment under hypoxia conditions, the complexes were removed and replaced with the complete medium and the cells were cultured for another 24 or 48 hr under hypoxia

conditions. The MTT assay was used to determine the cell viability 48 hr and 72 hr post transfection based on the manufacturer's protocol. Briefly, 10 μL of the MTT reagent was added into each well and the samples were incubated in a cell incubator at 37°C for 4 hr, and 100 μL of the SDS solution was then added into each well. Following another 8-hr incubation, absorbance of the samples was measured at 570 nm using a microplate reader (Spectramax M2 Multi-Mode microplate reader, Molecular Devices, LLC, San Jose, CA). Each complex was tested in triplicate. Cell viability was calculated based on the equation (2) below:

$$Cell\ viability(\%) = \left(\frac{OD_{sample}}{OD_{control}}\right) \times 100\% \quad (2)$$

## 2.6. Cellular uptake study

Cellular uptake of Chi/FAM-siRNA complexes with and without HA coating was studied using flow cytometry. MP-38 cells ($5\times10^5$ cells/well) were seeded in a 6-well plate and treated with FAM-siRNA complexes with different C/N/P ratios for different duration under hypoxia conditions at 37°C. The cells were periodically collected with the trypsin-EDTA reagent, fixed with 2% paraformaldehyde, and washed with FACs buffer (2% FBS in PBS). Relative mean fluorescence intensity (MFI) was the fold change comparing with non-treated cells. MFI of MP-38 cells was analyzed by a BD FACSVerse flow cytometer system (BD Bioscience, San Jose, CA).

A confocal laser scanning microscopy (CLSM, Nikon Eclipse Ti2 inverted confocal microscope, Tokyo, Japan) was used to visualize cellular uptake of the complexes. MP-38 cells were seeded into a 35 mm petri dish with 14 mm glass bottom microwell ($5\times10^5$ cells/petri dish) (MatTek Coporation Ashland, MA) and cultured at 37°C to reach 80% confluency. Then the cells were washed with PBS and treated with FAM-siRNA complexes (67 nM) in serum free media under hypoxic conditions. Following the treatment for different duration, the cells were labeled with LysoTracker Red DND-99 (50 nM) for 1 hr under hypoxic conditions. For qualitative observation of cellular uptake, MP-38 cells were fixed with 3.7% paraformaldehyde and the nuclei were stained with Hoechst 33342 for 10 min. The samples were then evaluated via CLSM.

## 2.7. RT-qPCR study of HIF-1α mRNA level expression

HIF-1α mRNA level expression following the treatment of siRNA complexes was investigated using Applied Biosystems Viia7 qPCR (Thermo Fisher Scientific, Waltham, MA). MP-38 cells were seeded in a 6-well plate with a cell density of $5\times10^5$ per well. After reaching approximately 80% confluency, the Chi/siRNA complexes with different C/N/P ratios (67 nM siRNA) were used to treat the cells. After the 24-hr treatment, the complexes were removed and replaced with the complete culture medium. 48-hr post transfection, the total RNA was isolated using the TRIzol reagent and reverse transcribed into cDNA using SuperScript™ IV First-Strand Synthesis System. The primer used was a Taqman™ Gene Expression Assay (FAM), GAPDH (Hs02786624_g1) and HIF-1α (Hs00153153_m1). HIF-1α mRNA level was normalized to the housekeeping gene GAPDH. Relative

quantification was done using $2^{-\Delta\Delta^{CT}}$ method, in which the control was normalized for percent fold changes.

### 2.8. Western blot study of HIF-1α protein expression

The siRNA-mediated expression reduction of the target protein HIF-1α was assessed using Western Blotting. Following the treatment of Chi/siRNA complexes for 72 hr, the MP-38 cells were immediately washed with ice-cold PBS and lysates were harvested using a M-PER™ Mammalian Protein Extraction Reagent with 1% protease inhibitor. The total protein concentration was determined by Pierce™ BCA Protein Assay Kit. The whole cell lysates (20 μg total protein) were separated by SDS-PAGE on a 4–20% Mini-PROTEAN gel and transferred to 0.45 μm Immobilion®-P PVDF transfer membrane. The membranes were incubated with primary antibodies, mouse anti-human HIF-1α monoclonal antibody (1:2,000), mouse anti-human VEGF monoclonal antibody (1:1,000), and mouse anti-human GAPDH monoclonal antibody (1:10,000) overnight at 4°C. The anti-mouse IgG, HRP-linked antibody was used as the secondary antibody and applied in blots for 1 hr at room temperature. The blot images were taken following the SuperSignal™ West Pico PLUS Chemiluminescent substrate protocol (Thermo Scientific).

### 2.9. *In* vitro migration and invasion studies

*In vitro* cell migration and invasion assays were conducted to assess whether the produced siRNA complexes can inhibit the migration and invasion of UM cells. For the cell migration assay, MP-38 cells were treated with the HIF-1α siRNA complexes with or without HA coating for 24 hr in a hypoxia chamber. After the incubation, the MP-38 cells ($1\times10^5$ cells/well) were collected in the serum free RPMI-1640 medium and placed in the upper chamber of a Transwell® insert. The inserts were then placed on a 24-well plate. 500 μL of PRMI-1640 medium containing 20% FBS was placed in the lower chamber of the plate to act as a chemo-attractant. The cells were incubated under hypoxic conditions for 24 hr and fixed with 75% ethanol and stained with 0.2% crystal violet. The non-migrated cells remaining in the upper chamber of the inserts were gently removed using cotton swabs. The migrated cells attached to the bottom surface of the Transwell® membrane were observed using EVOS® FL Auto Cell Imaging System (Thermo Fisher Waltham, MA).

For the invasion assay, the Transwell® insert membrane was coated with 40 μL of Matrigel® (0.125 mg/mL) for 4 hr before seeding MP-38 cells. After the transfection with the siRNA complexes for 24 hr, the MP-38 cells ($1 \times 10^5$ cells/well) were placed in the upper chamber of the Transwell® plate with serum free PRMI-1640 medium. Fibroblasts-conditioned medium (DMEM medium containing 10% FBS used to grow NIH3T3 fibroblast cells) was added into to the lower chamber of the Transwell® plate as the chemoattractant (Justus et al., 2014). After incubation under hypoxic conditions for 24 hr, the MP-38 cells were fixed, stained, and studied using the same method as described above in the migration study.

### 2.10. Statistical analysis

All data were collected and presented as average ± SD (standard deviation). The statistical significance was determined using Student's *t*-test with $p<0.05$ as the minimal level of significance.

## 3. RESULTS AND DISCUSSION

### 3.1. Characteristics of siRNA complexes

The positive charge in the Chi backbone makes it easy for Chi to interact with negatively charged siRNA, to form nanosized complexes via electrostatic interaction (Howard et al., 2006; Katas and Alpar, 2006). As shown in Table 1, the hydrodynamic diameter ($D_H$) of all siRNA complexes were below 200 nm. The binary complexes with a N/P molar ratio of 40/1 had smaller particle size (174.3 ± 7.72 nm) and PDI (0.26 ± 0.013) than that of the complexes with a N/P molar ratio of 20/1 (195.6 ± 2.55 nm, PDI: 0.38 ± 0.023), which was consistent with the previous finding (Mao et al., 2010). High N/P ratio provides more Chi-siRNA bond-forming bridges, leading to greater chitosan incorporation in the core of the complexes and hence smaller particle size (Howard et al., 2006). The binary Chi/siRNA complexes were positively charged (~13 mV). The surface charge of the complexes changed from positive to negative (~−16 mV to −24 mV) after coated with HA at various C/P ratios, which suggested the successful coating of polyanion HA. Compared to the respective binary siRNA complexes, HA coating resulted in an increased particle size for the complexes with a N/P ratio of 40/1, whereas a significantly decreased particle size for the complexes with a N/P ratio of 20/1 ($p<0.01$) (Table 1). It is believed that the HA chain can be not only located in the outer coating layer, but also integrated into the bulk complex structure via electrostatic interaction (Lallana et al., 2017). For the complexes with a higher N/P ratio (40/1), the formed binary complexes were tightly condensed and thereby, less chance of HA being integrated into the core structure of the complex than forming an outer coating layer, resulting in an increase in particle size. On the other hand, the complexes with a lower N/P ratio (20/1) had a less condensed core structure, thus a higher chance of HA being integrated into the core structure of the binary complex to form ternary complexes with decreased particle size. Overall, increasing the amount of HA coating did not appear to impact particle size of the complexes, indicating that a plateau may have reached (Duceppe and Tabrizian, 2009). The control group (DF-siRNA) was positively charged (~49 mV) with a particle size of 192 nm.

TEM images show that all produced siRNA complexes had a round shape, and the images of representative siRNA complexes (N/P ratio: 40/1) are shown in Figure 1. The particle size observed via TEM was smaller (below 150 nm), compared to that obtained using DLS. The drying procedure during TEM sample preparation may lead to shrinkage of the complexes and thereby smaller particle size (Biro et al., 2008; Duceppe and Tabrizian, 2009).

The siRNA loading efficiency of the complexes were studied using agarose gel electrophoresis. The free siRNA detected from all complexes or DF-siRNA suspensions was compared with the control group (naked siRNA) (Figure 2). Based on equation (1), the siRNA loading efficiency of each complex formulation was calculated. As shown in Table 1,

the siRNA loading efficiency in all complexes was above 80%, indicating that all complexes can condense siRNA efficiently. The complexes with a high N/P molar ratio (40/1) had a similar siRNA loading efficiency (~90%) to the commercial reagent DF. Moreover, the HA coating did not appear to affect siRNA loading in the complex formulations. All our complex formulations can protect siRNA from RNase A degradation compared to the naked siRNA (Figure 3A). The semiquantitative results confirmed that significantly higher siRNA remained in the complex groups compared to the naked siRNA (Figure 3B) ($p<0.05$), indicating that the developed ternary complex is a stable siRNA delivery system.

### 3.2. Cytotoxicity of siRNA complexes

The cell viability at 48 hr (black bar) and 72 hr (gray bar) following the treatment of siRNA complexes under hypoxia conditions are shown in Figures 4A and 4B. All Chi/HIF-1α siRNA complexes (with or without HA coating) showed decreased cell viability compared with the untreated control group. The complexes with a higher Chi or HA amount (a higher N/P or C/P ratio) appeared to have higher toxicity against MP-38 cells at both 48 and 72 hr (Figure 4A). However, the complexes loaded with scramble siRNA and polymer solution controls showed low toxicity to MP38 cells, and the cell viability was in the range of 85% to 98% compared to the untreated control group (Figure 4B). This suggested that the decreased cell viability may result from the successful inhibition of HIF-1α gene expression that affects cell proliferation under low oxygen environment (Rankin and Giaccia, 2016; Semenza, 2012). Although the cells treated with the HA and low concentration Chi solutions had slightly decreased viability at 48 hr, the cell viability was recovered at 72 hr. However, the high concentration Chi solution didn't show good cell viability at 72 hr. This could be explained by increased cytotoxicity associated with high concentration polycations. The commercial product DF did not affect cell viability under hypoxia conditions when loaded with scrambled siRNAs. Whereas, HIF-1α siRNA loaded DF showed similar cell viability to the complex groups (C/N/P: 20/40/1 and 40/40/1) at 72 hr.

### 3.3. Cellular uptake of siRNA complexes

The cellular uptake of Chi/FAM-siRNA complexes (with or without HA coating) into MP-38 cells was investigated under hypoxic conditions for 4 hr. As shown in Figure 5A, cellular uptake of the developed siRNA complexes in MP38 cells was drastically improved compared to that of the naked FAM-siRNA. Moreover, the developed siRNA complexes (except for the complex with a C/N/P ratio of 20/40/1) showed significantly higher cellular uptake than the commercial delivery reagent (DF) ($p<0.05$). The amount of HA coating appeared to play an important role in cellular uptake of the produced complexes. The ternary complexes with a high HA amount (C/P: 40/1) showed the best cellular uptake. HA is a well-known ligand for CD44 receptor that is strongly expressed in UM (Danen et al., 1996). Therefore, a high amount of HA coating (C/P: 40/1) can lead to enhanced receptor-mediated endocytosis, thus better cellular uptake (Zaki et al., 2011). However, when the HA coating amount was low (C/P: 20/1), the binary complexes showed better cellular uptake than the ternary complexes. This can be explained by strong electrostatic interactions between positively charged binary siRNA complexes and MP38 cells (Harush-Frenkel et al., 2007; Harush-Frenkel et al., 2008; Huang et al., 2004; Zaki et al., 2011). HA coating shielded the positive charge of the binary siRNA complexes (Table 1), impeding the electrostatic

interactions between the complexes and MP38 cells. Among all the complexes investigated, the ternary complex with a C/N/P ratio of 40/40/1 showed the best cellular uptake (6.26 ± 0.58 fold higher than the non-treated control group).

A cellular uptake time course study of the ternary complex (C/N/P: 40/40/1) was then conducted. The binary complex (N/P: 40/1) and commercial delivery reagent (DF) were studied as controls. The cellular uptake of the ternary siRNA complexes showed a time-dependent manner, and the fluorescence signal drastically increased from 1 hr to 4 hr for all the complexes studied (Figure 5B). After the 4-hr treatment, the Chi/FAM-siRNA complexes with and without HA coating showed 2.01 and 1.45 fold higher relative MFI in comparison to DF, respectively. More importantly, the ternary siRNA complexes (C/N/P: 40/40/1) showed significantly higher FAM intensity compared to the binary complex ($p<0.001$) and DF groups ($p<0.001$).

In order to elucidate the intracellular trafficking process of the developed siRNA complexes, Lysotracker™ (red) was used to stain lysosome. As shown in Figures 6A and 6B, most FAM signal (green) overlapped with Lysotracker™ signal (red) in MP-38 cells at 1 hr for the complexes with or without HA coating (N/P: 40/1). With increasing incubation time, strong FAM signal (green) appeared around the Lysotracker™ signal (red) and most FAM signal (green) was outside the Lysotracker™ area (red) after the 4-hr incubation, suggesting that the developed siRNA complexes can escape from lysosome. The Z-stack CLMS image confirmed that most siRNA and lysosome inside MP-38 cells were not overlapped in the Z direction 2 hr and 4 hr posttreatment for the binary (N/P: 40/1) and ternary (C/N/P: 40/40/1) complex groups as well as the DF-siRNA group (Figure 6C). Our results demonstrated that chitosan complexes can have fast internalization and endosomal escape process, which was consistent with the literature report (Zaki et al., 2011). This may be resulted from the “proton sponge” effect associated with excess polycation Chi, which can lyse vesicle entrapment of the polyplex and protect siRNA from degradation in lysosome (Lechardeur et al., 2005; Mao et al., 2001). More importantly, the HA coating did not affect the endosomal escape ability of the chitosan-based siRNA complexes. DF, a commercially available cationic lipid based delivery system, showed endosomal escape ability as well (Figure 6C). However, the fluorescence signal of the DF-siRNA group was not as strong as that of our complex formulations at both 2 and 4 hr, which was consistent with the cellular uptake results determined using flow cytometer (Figure 5B). These results confirmed that the developed siRNA complexes can successfully deliver siRNA into MP38 cells and possess excellent lysosome escape ability.

### 3.4. Inhibition of HIF-1α mRNA expression

We studied HIF-1α silencing efficiency of the developed siRNA complexes under hypoxia conditions. As shown in Figure 7, the siRNA complexes (with or without HA coating) at a N/P ratio of 40/1, showed a significant decrease in HIF-1α mRNA expression level compared to scramble siRNA complexes ($p<0.05$). In the case of low N/P ratio (20/1) groups, only the ternary complex with high HA coating (C/N/P: 40/20/1) showed significant HIF-1α gene knockdown efficiency ($p<0.05$). High HA coating (C/P: 40/1) resulted in high cellular uptake (Figure 5) and consequently, better HIF-1α knockdown effect. Moreover, the

polyanionic HA can loosen the tight Chi-siRNA binding, which may promote siRNA release from the complexes, thus improving siRNA silencing effect (Al-Qadi et al., 2013). When comparing all produced siRNA complexes with the DF-siRNA group, the ternary siRNA complex (C/N/P, 40/40/1) and DF-siRNA groups had significantly lower HIF-1α mRNA expression compared to other siRNA complex groups ($p<0.05$), and there was no significant difference observed between these two groups ($p>0.05$) (Figure 7).

### 3.5. Downregulation of HIF-1α protein expression

As shown in Figures 8A and 8B, complexes treated MP-38 cells had HIF-1α protein expression ranging from 55.0% to 85.5% relative to the control. The complexes with high HA coating (C/N/P: 40/20/1 and 40/40/1) showed the best HIF-1α protein downregulation efficiency (55.1% ± 6.41 and 56.3% ± 5.45%, respectively), which was lower than the commercial siRNA delivery reagent DF (62.0% ± 5.61%) ($p>0.05$). In addition, the complexes (C/N/P, 40/40/1) showed significantly lower HIF-1α protein level compared to the complexes without HA coating (C/N/P, 0/40/1) ($p<0.05$). The excellent gene knockdown effect of the ternary siRNA complexes with high HA coating can be attributed to good cellular uptake as demonstrated in Figure 5A. The HIF-1α expression is known to be strongly associated with vascular markers in UM (Mouriaux et al., 2014). Accordingly, we also evaluated VEGF protein expression level in MP-38 cells following the treatment of the developed siRNA complexes. As shown in Figures 8A and 8C, VEGF expression was decreased after the treatment of the siRNA complexes, following a similar trend to the HIF-1α protein expression. The ternary complexes with high HA coating (C/N/P: 40/20/1 and 40/40/1) resulted in 47.4% ± 7.58% and 46.8% ± 2.87% VEGF protein expression relative to the control, which was slightly lower than the DF-siRNA group (49.6% ± 9.12%). HIF-1α is a central transcription regulator of VEGF expression induced by hypoxia response (Carmeliet et al., 1998; Moritz et al., 2002). Therefore, downregulation of HIF-1α expression resulted in decreased VEGF expression.

### 3.6. *In vitro* UM migration and invasion

To demonstrate whether the developed siRNA complexes can inhibit metastasis of MP-38 cells, we evaluated UM cell migration and invasion under hypoxia conditions. As shown in Figure 9, untreated MP cells were not able to migrate or invade through the transwell membrane without the presence of a chemoattractant (e.g. FBS or the complete medium used for culturing NIH3T3 fibroblast cells). In the presence of the chemoattractants, MP-38 cells treated with HIF-1a siRNA-loaded complexes, particularly the ones with high HA coating (C/P: 40/1), showed significant suppression of UM migration and invasion under hypoxia conditions, compared to the untreated control group. Both HIF-1a and VEGF expression have been shown to be critical for tumorigenesis and UM metastasis (Martinengo et al., 2014; Tang et al., 2004). Therefore, downregulation of HIF-1α expression and subsequent VEGF expression as demonstrated in Figure 8, resulted in successful inhibition of UM migration and invasion.

Introducing the molecularly targeted therapy based on the developed anti-HIF-1a siRNA complexes in the posterior eye segment as early as possible, could be critical to prevent UM metastasis, thus improving UM prognosis and survival, particularly when aggressive

treatment (e.g. enucleation and irradiation) is not an “immediate” treatment option. In addition, the HA coating is expected to not only improve cellular uptake but also facilitate the complex transport in the vitreous humor. In future studies, the ternary siRNA complexes *via* intravitreal administration will be tested using an UM mouse model.

## 4. CONCLUSIONS

We have developed a novel molecularly targeted therapeutic strategy based on biocompatible ternary siRNA complexes for the treatment of UM, the most common and malignant primary intraocular tumor in adults. The developed ternary siRNA complexes were below 190 nm in size and negatively charged, and had above 80% siRNA loading efficiency. Owing to the combination effect of HA and chitosan, the ternary complexes demonstrated improved cellular uptake and lysosomal escape ability. In addition, we have shown that the developed ternary complexes successfully inhibited HIF-1α expression in both mRNA and protein levels under hypoxia conditions, which subsequently downregulated VEGF protein expression. As a result, UM migration and invasion were suppressed. These results indicated that the developed ternary complexes have the potential to inhibit UM metastases, opening a new venue for UM treatment.

## ACKNOWLEDGEMENT

This work was fully supported by the Institutional Development Award (IDeA) Network for Biomedical Research Excellence from the National Institute of General Medical Sciences of the National Institutes of Health under grant number P20GM103430.

## Biography

**Lingxiao Xie:** Conceptualization; Methodology; Validation; Formal analysis; Investigation; Data Curation; Writing - Original Draft; Writing - Review & Editing; Visualization.

**Yan Yang:** Formal analysis; Writing - Review & Editing.

**Jie Shen:** Conceptualization; Resources; Writing - Review & Editing; Visualization; Supervision, Project administration, Funding acquisition.

## REFERENCE

Al-Qadi S, Alatorre-Meda M, Zaghloul EM, Taboada P, Remunan-Lopez C, 2013 Chitosan-hyaluronic acid nanoparticles for gene silencing: the role of hyaluronic acid on the nanoparticles’ formation and activity. Colloids Surf B Biointerfaces 103, 615–623. [PubMed: 23274155]

Amirouchene-Angelozzi N, Schoumacher M, Stern MH, Cassoux N, Desjardins L, Piperno-Neumann S, Lantz O, Roman-Roman S, 2015 Upcoming translational challenges for uveal melanoma. Br J Cancer 113, 1746.

Asnaghi L, Lin MH, Lim KS, Lim KJ, Tripathy A, Wendeborn M, Merbs SL, Handa JT, Sodhi A, Bar EE, Eberhart CG, 2014 Hypoxia promotes uveal melanoma invasion through enhanced Notch and MAPK activation. Plos One 9, e105372. [PubMed: 25166211]

Bhatia S, Moon J, Margolin KA, Weber JS, Lao CD, Othus M, Aparicio AM, Ribas A, Sondak VK, 2012 Phase II trial of sorafenib in combination with carboplatin and paclitaxel in patients with metastatic uveal melanoma: SWOG S0512. PLoS One 7, e48787. [PubMed: 23226204]

Biro E, Nemeth AS, Sisak C, Feczko T, Gyenis J, 2008 Preparation of chitosan particles suitable for enzyme immobilization. J Biochem Biophys Methods 70, 1240–1246. [PubMed: 18155771]

Carmeliet P, Dor Y, Herbert JM, Fukumura D, Brusselmans K, Dewerchin M, Neeman M, Bono F, Abramovitch R, Maxwell P, Koch CJ, Ratcliffe P, Moons L, Jain RK, Collen D, Keshert E, 1998 Role of HIF-1alpha in hypoxia-mediated apoptosis, cell proliferation and tumour angiogenesis. Nature 394, 485–490. [PubMed: 9697772]

Carvajal RD, Schwartz GK, Tezel T, Marr B, Francis JH, Nathan PD, 2017 Metastatic disease from uveal melanoma: treatment options and future prospects. Br J Ophthalmol 101, 38–44. [PubMed: 27574175]

Damato B, 2006 Treatment of primary intraocular melanoma. Expert Rev Anticancer Ther 6, 493–506. [PubMed: 16613538]

Danen EH, ten Berge PJ, van Muijen GN, Jager MJ, Ruiter DJ, 1996 Expression of CD44 and the pattern of CD44 alternative splicing in uveal melanoma. Melanoma Res 6, 31–35. [PubMed: 8640067]

Dehousse V, Garbacki N, Jaspart S, Castagne D, Piel G, Colige A, Evrard B, 2010 Comparison of chitosan/siRNA and trimethylchitosan/siRNA complexes behaviour in vitro. Int J Biol Macromol 46, 342–349. [PubMed: 20096725]

Diener-West M, Hawkins BS, Markowitz JA, Schachat AP, 1992 A review of mortality from choroidal melanoma. II. A meta-analysis of 5-year mortality rates following enucleation, 1966 through 1988. Arch Ophthalmol 110, 245–250. [PubMed: 1531290]

Duceppe N, Tabrizian M, 2009 Factors influencing the transfection efficiency of ultra low molecular weight chitosan/hyaluronic acid nanoparticles. Biomaterials 30, 2625–2631. [PubMed: 19201022]

Gao S, Chen J, Dong L, Ding Z, Yang YH, Zhang J, 2005 Targeting delivery of oligonucleotide and plasmid DNA to hepatocyte via galactosylated chitosan vector. Eur J Pharm Biopharm 60, 327–334. [PubMed: 15894474]

Ghosh K, Pan Z, Guan E, Ge S, Liu Y, Nakamura T, Ren XD, Rafailovich M, Clark RA, 2007 Cell adaptation to a physiologically relevant ECM mimic with different viscoelastic properties. Biomaterials 28, 671–679. [PubMed: 17049594]

Hanna SC, Krishnan B, Bailey ST, Moschos SJ, Kuan PF, Shimamura T, Osborne LD, Siegel MB, Duncan LM, O'Brien ET 3rd, Superfine R, Miller CR, Simon MC, Wong KK, Kim WY, 2013 HIF1alpha and HIF2alpha independently activate SRC to promote melanoma metastases. J Clin Invest 123, 2078–2093. [PubMed: 23563312]

Harbour JW, 2012 The genetics of uveal melanoma: an emerging framework for targeted therapy. Pigment Cell Melanoma Res 25, 171–181. [PubMed: 22268848]

Harush-Frenkel O, Debotton N, Benita S, Altschuler Y, 2007 Targeting of nanoparticles to the clathrin-mediated endocytic pathway. Biochem Biophys Res Commun 353, 26–32. [PubMed: 17184736]

Harush-Frenkel O, Rozentur E, Benita S, Altschuler Y, 2008 Surface charge of nanoparticles determines their endocytic and transcytotic pathway in polarized MDCK cells. Biomacromolecules 9, 435–443. [PubMed: 18189360]

Hiraga T, Kizaka-Kondoh S, Hirota K, Hiraoka M, Yoneda T, 2007 Hypoxia and hypoxia-inducible factor-1 expression enhance osteolytic bone metastases of breast cancer. Cancer Res 67, 4157–4163. [PubMed: 17483326]

Howard KA, Rahbek UL, Liu X, Damgaard CK, Glud SZ, Andersen MO, Hovgaard MB, Schmitz A, Nyengaard JR, Besenbacher F, Kjems J, 2006 RNA interference in vitro and in vivo using a novel chitosan/siRNA nanoparticle system. Mol Ther 14, 476–484. [PubMed: 16829204]

Hu K, Babapoor-Farrokhran S, Rodrigues M, Deshpande M, Puchner B, Kashiwabuchi F, Hassan SJ, Asnaghi L, Handa JT, Merbs S, Eberhart CG, Semenza GL, Montaner S, Sodhi A, 2016 Hypoxia-inducible factor 1 upregulation of both VEGF and ANGPTL4 is required to promote the angiogenic phenotype in uveal melanoma. Oncotarget 7, 7816–7828. [PubMed: 26761211]

Huang M, Khor E, Lim LY, 2004 Uptake and cytotoxicity of chitosan molecules and nanoparticles: effects of molecular weight and degree of deacetylation. Pharm Res 21, 344–353. [PubMed: 15032318]

Justus CR, Leffler N, Ruiz-Echevarria M, Yang LV, 2014 In vitro cell migration and invasion assays. J Vis Exp.

Kaliki S, Shields CL, 2016 Uveal melanoma: relatively rare but deadly cancer. Eye (Lond).

Katas H, Alpar HO, 2006 Development and characterisation of chitosan nanoparticles for siRNA delivery. J Control Release 115, 216–225. [PubMed: 16959358]

Lallana E, Rios de la Rosa JM, Tirella A, Pelliccia M, Gennari A, Stratford IJ, Puri S, Ashford M, Tirelli N, 2017 Chitosan/Hyaluronic Acid Nanoparticles: Rational Design Revisited for RNA Delivery. Mol Pharm 14, 2422–2436. [PubMed: 28597662]

Lechardeur D, Verkman AS, Lukacs GL, 2005 Intracellular routing of plasmid DNA during non-viral gene transfer. Adv Drug Deliv Rev 57, 755–767. [PubMed: 15757759]

Liao D, Corle C, Seagroves TN, Johnson RS, 2007 Hypoxia-inducible factor-1alpha is a key regulator of metastasis in a transgenic model of cancer initiation and progression. Cancer Res 67, 563–572. [PubMed: 17234764]

MacLaughlin FC, Mumper RJ, Wang J, Tagliaferri JM, Gill I, Hinchcliffe M, Rolland AP, 1998 Chitosan and depolymerized chitosan oligomers as condensing carriers for in vivo plasmid delivery. J Control Release 56, 259–272. [PubMed: 9801449]

Mansouri S, Lavigne P, Corsi K, Benderdour M, Beaumont E, Fernandes J.C.J.E.j.o.p., biopharmaceutics, 2004 Chitosan-DNA nanoparticles as non-viral vectors in gene therapy: strategies to improve transfection efficacy. European journal of pharmaceutics 57, 1–8.

Mao H-Q, Roy K, Troung-Le VL, Janes KA, Lin KY, Wang Y, August JT, Leong KW, 2001 Chitosan-DNA nanoparticles as gene carriers: synthesis, characterization and transfection efficiency. Journal of controlled release 70, 399–421. [PubMed: 11182210]

Mao S, Sun W, Kissel T, 2010 Chitosan-based formulations for delivery of DNA and siRNA. Adv Drug Deliv Rev 62, 12–27. [PubMed: 19796660]

Martens TF, Remaut K, Deschout H, Engbersen JF, Hennink WE, van Steenbergen MJ, Demeester J, De Smedt SC, Braeckmans K, 2015 Coating nanocarriers with hyaluronic acid facilitates intravitreal drug delivery for retinal gene therapy. J Control Release 202, 83–92. [PubMed: 25634806]

Martinengo C, Poggio T, Menotti M, Scalzo MS, Mastini C, Ambrogio C, Pellegrino E, Riera L, Piva R, Ribatti D, Pastorino F, Perri P, Ponzoni M, Wang Q, Voena C, Chiarle R, 2014 ALK-dependent control of hypoxia-inducible factors mediates tumor growth and metastasis. Cancer Res 74, 6094–6106. [PubMed: 25193384]

Moritz W, Meier F, Stroka DM, Giuliani M, Kugelmeier P, Nett PC, Lehmann R, Candinas D, Gassmann M, Weber M, 2002 Apoptosis in hypoxic human pancreatic islets correlates with HIF-1alpha expression. Faseb J 16, 745–747. [PubMed: 11923216]

Moser JC, Pulido JS, Dronca RS, McWilliams RR, Markovic SN, Mansfield AS, 2015 The Mayo Clinic experience with the use of kinase inhibitors, ipilimumab, bevacizumab, and local therapies in the treatment of metastatic uveal melanoma. Melanoma Res 25, 59–63. [PubMed: 25396683]

Mouriaux F, Sanschagrin F, Diorio C, Landreville S, Comoz F, Petit E, Bernaudin M, Rousseau AP, Bergeron D, Morcos M, 2014 Increased HIF-1alpha expression correlates with cell proliferation and vascular markers CD31 and VEGF-A in uveal melanoma. Invest Ophthalmol Vis Sci 55, 1277–1283. [PubMed: 24481264]

Munzenrider JE, 2001 Uveal melanomas. Conservation treatment. Hematol Oncol Clin North Am 15, 389–402. [PubMed: 11370500]

Onken MD, Li J, Cooper JA, 2014 Uveal melanoma cells utilize a novel route for transendothelial migration. Plos One 9, e115472. [PubMed: 25506912]

Rankin EB, Giaccia AJ, 2016 Hypoxic control of metastasis. Science 352, 175–180. [PubMed: 27124451]

Semenza GL, 2012 Hypoxia-inducible factors in physiology and medicine. Cell 148, 399–408. [PubMed: 22304911]

Shields CL, Furuta M, Thangappan A, Nagori S, Mashayekhi A, Lally DR, Kelly CC, Rudich DS, Nagori AV, Wakade OA, Mehta S, Forte L, Long A, Dellacava EF, Kaplan B, Shields JA, 2009 Metastasis of uveal melanoma millimeter-by-millimeter in 8033 consecutive eyes. Arch Ophthalmol 127, 989–998. [PubMed: 19667335]

Spagnolo F, Caltabiano G, Queirolo P, 2012 Uveal melanoma. Cancer Treat Rev 38, 549–553. [PubMed: 22270078]

Tang N, Wang L, Esko J, Giordano FJ, Huang Y, Gerber H-P, Ferrara N, Johnson R.S.J.C.c., 2004 Loss of HIF-1α in endothelial cells disrupts a hypoxia-driven VEGF autocrine loop necessary for tumorigenesis. 6, 485–495.

Wong CC-L, Gilkes DM, Zhang H, Chen J, Wei H, Chaturvedi P, Fraley SI, Wong C-M, Khoo U-S, Ng I.O.-LJ.P.o.t.N.A.o.S., 2011 Hypoxia-inducible factor 1 is a master regulator of breast cancer metastatic niche formation. Proceedings of the National Academy of Sciences 108, 16369–16374.

Woodman SE, 2012 Metastatic uveal melanoma: biology and emerging treatments. Cancer J 18, 148–152. [PubMed: 22453016]

Xu Q, Boylan NJ, Suk JS, Wang YY, Nance EA, Yang JC, McDonnell PJ, Cone RA, Duh EJ, Hanes J, 2013 Nanoparticle diffusion in, and microrheology of, the bovine vitreous ex vivo. J Control Release 167, 76–84. [PubMed: 23369761]

Zaki NM, Nasti A, Tirelli N, 2011 Nanocarriers for cytoplasmic delivery: cellular uptake and intracellular fate of chitosan and hyaluronic acid-coated chitosan nanoparticles in a phagocytic cell model. Macromol Biosci 11, 1747–1760. [PubMed: 21954171]

Zhang H, Wong CC, Wei H, Gilkes DM, Korangath P, Chaturvedi P, Schito L, Chen J, Krishnamachary B, Winnard PT Jr., Raman V, Zhen L, Mitzner WA, Sukumar S, Semenza GL, 2012 HIF-1-dependent expression of angiopoietin-like 4 and L1CAM mediates vascular metastasis of hypoxic breast cancer cells to the lungs. Oncogene 31, 1757–1770. [PubMed: 21860410]

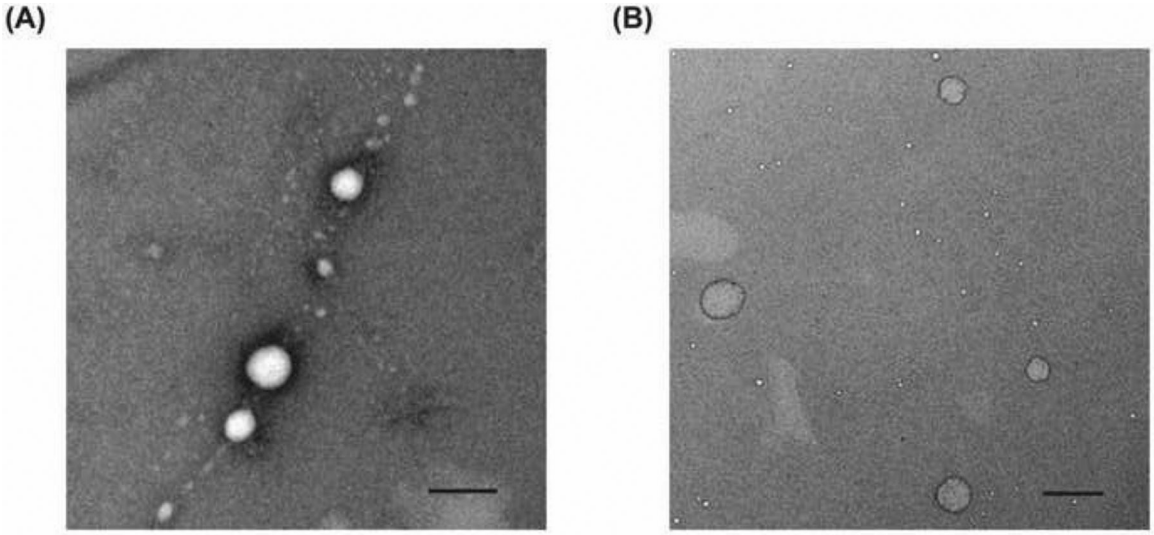


**Figure 1.**
TEM images of the Chi/siRNA complexes with C/N/P molar ratios of 0/40/1 (A) and 40/40/1 (B), respectively. Scale bar = 200 nm.

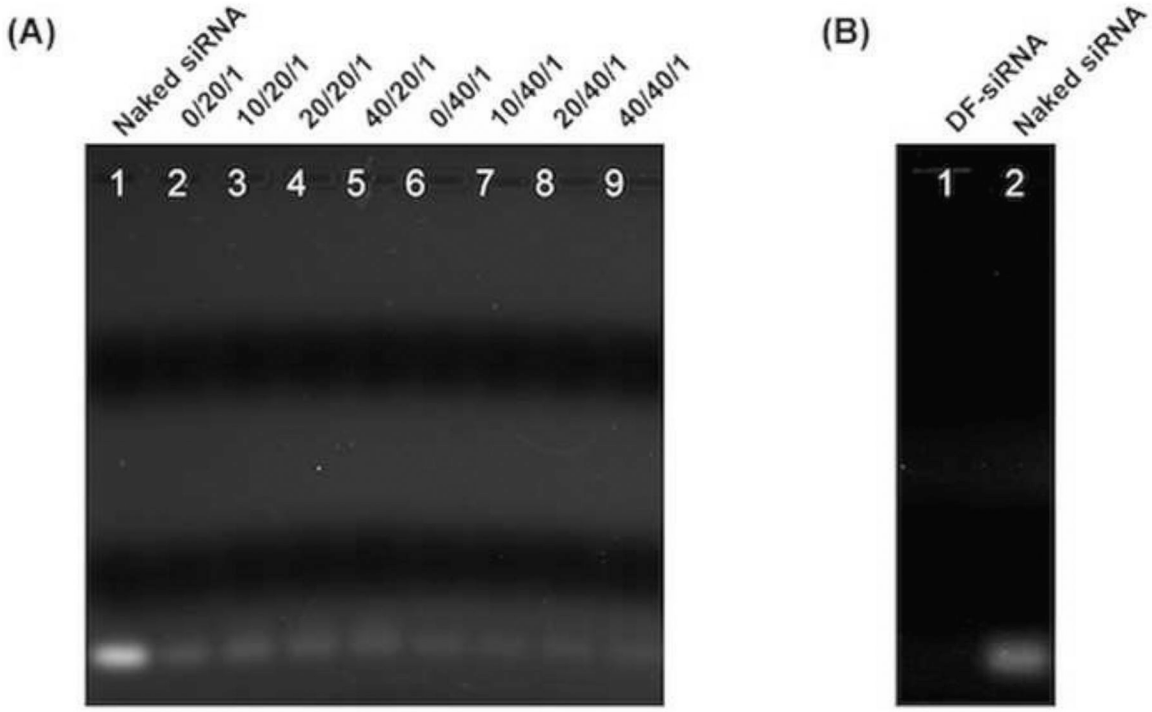


**Figure 2.**

Gel retardation assay of siRNA complexes with and without HA coating at various C/N/P ratios (A), and siRNA complexes with the commercial reagent DF (B). Naked siRNA (siRNA in a free form) was studied as control.

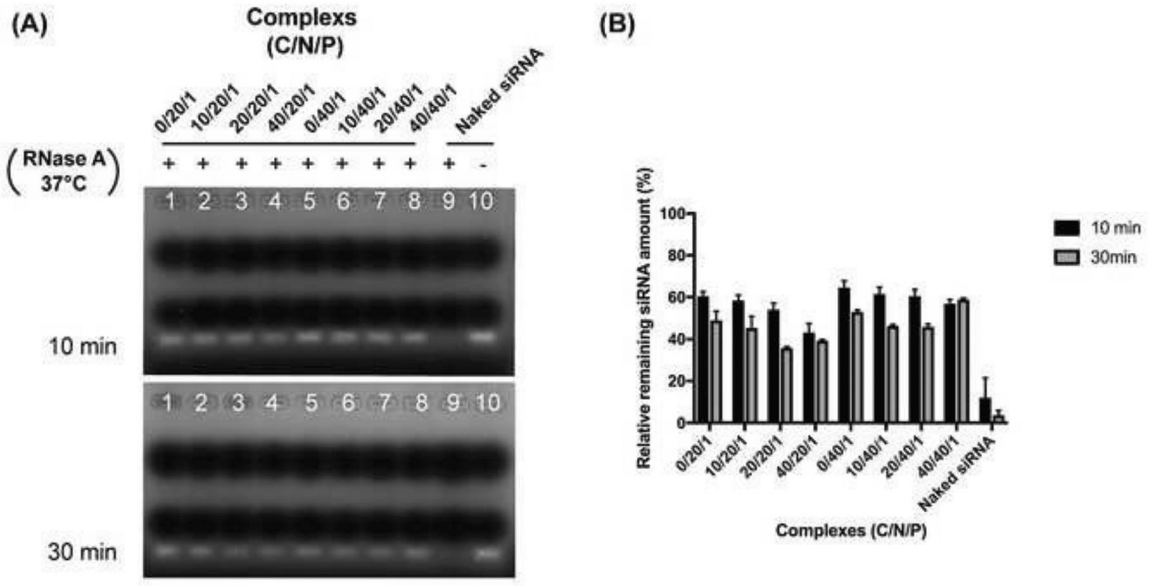


**Figure 3.**

(A) Agarose gel electrophoresis of Chi/siRNA and HA coated Chi/siRNA complexes after incubation with 0.01U/mg RNase A for 10 min and 30 min at 37°C. “+” represents the complexes incubated with RNase A at 37°C, “−” represents the same amount of siRNA without incubation with RNase A at 37°C. (B) Semi-quantification results of the complexes or naked siRNA following the co-incubation with RNase A.

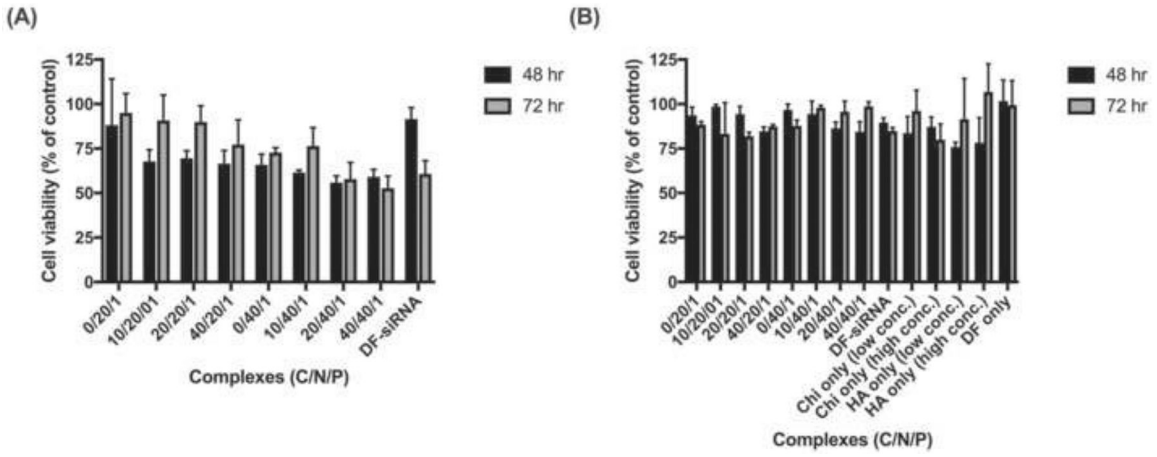


**Figure 4.**

MP38 cell viability after treated with HIF-1α siRNA-loaded complexes (A) and scramble siRNA-loaded complexes (B) for 48 and 72 hr under hypoxia conditions. Chitosan (Chi) solutions with the same concentrations as that used in the complexes with N/P ratios with 20/1 (low conc.) and 40/1 (high conc.), hyaluronic acid (HA) solutions with the same concentrations as that used in the ternary complexes with C/N/P ratios of 10/40/1 (low conc.) and 40/40/1 (high conc.), and a commercial agent DharmaFECT 1 (DF) were studied as controls.

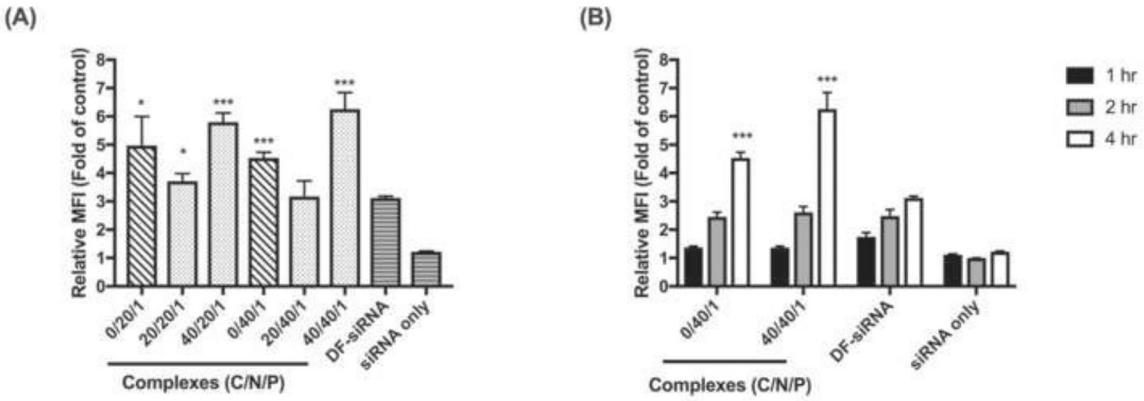


**Figure 5.**

Cellular uptake of FAM-siRNA complexes under hypoxia conditions at 4 hr (A) and the representative FAM-siRNA complexes at different time points (1, 2, and 4 hr) (B) in MP-38 cells determined using flow cytometry. The relative mean fluorescence (MFI) is the fold change compared to the no complexes or siRNA treated group. A commercial agent DharmaFECT 1 (DF) was studied as a control. Statistical analysis comparing the developed complexes to the DF group at the same time point. * $p<0.05$; *** $p<0.001$.

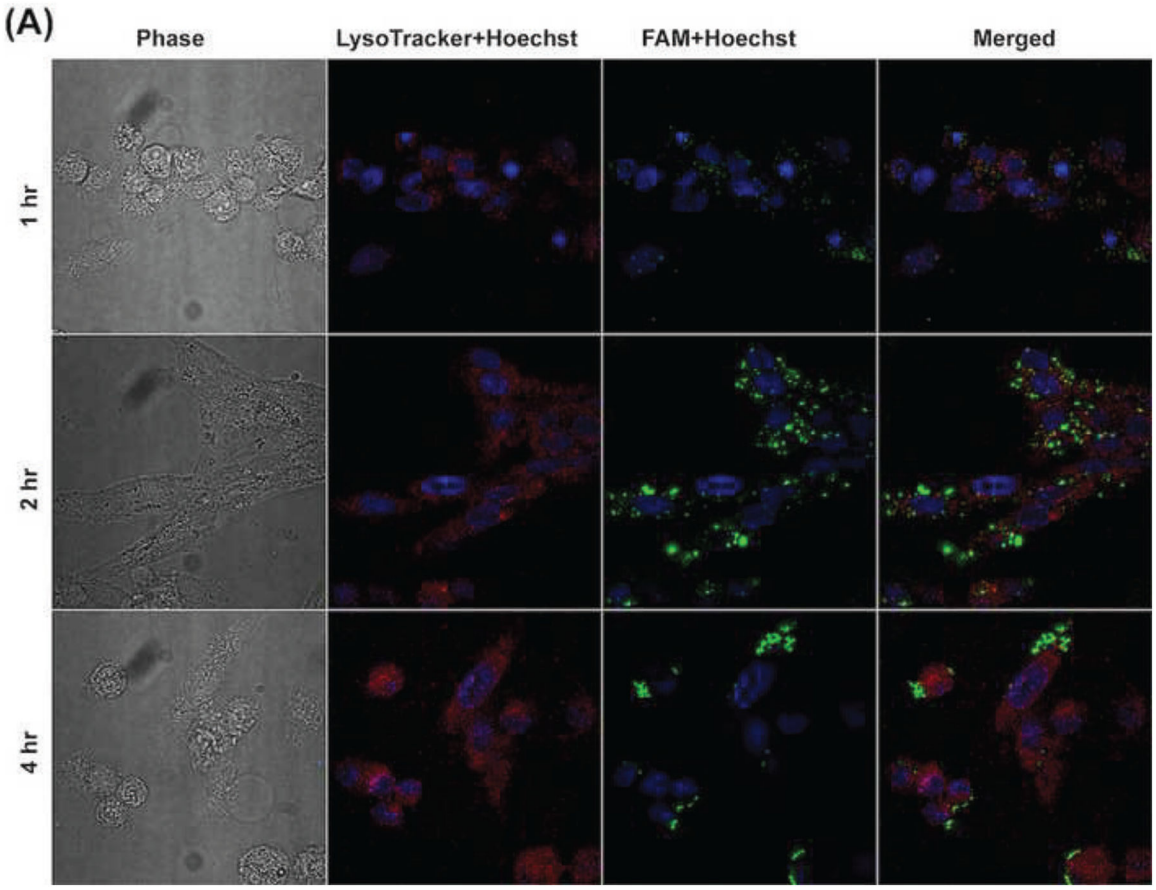

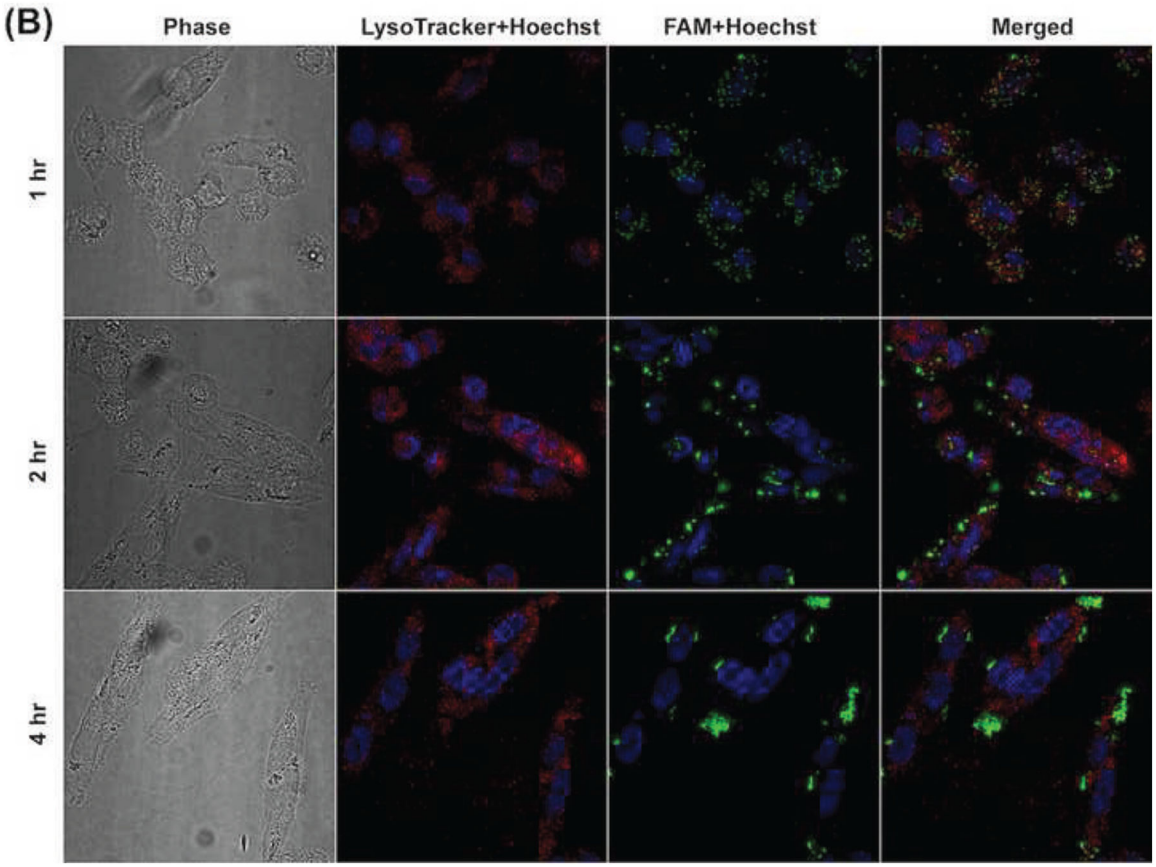

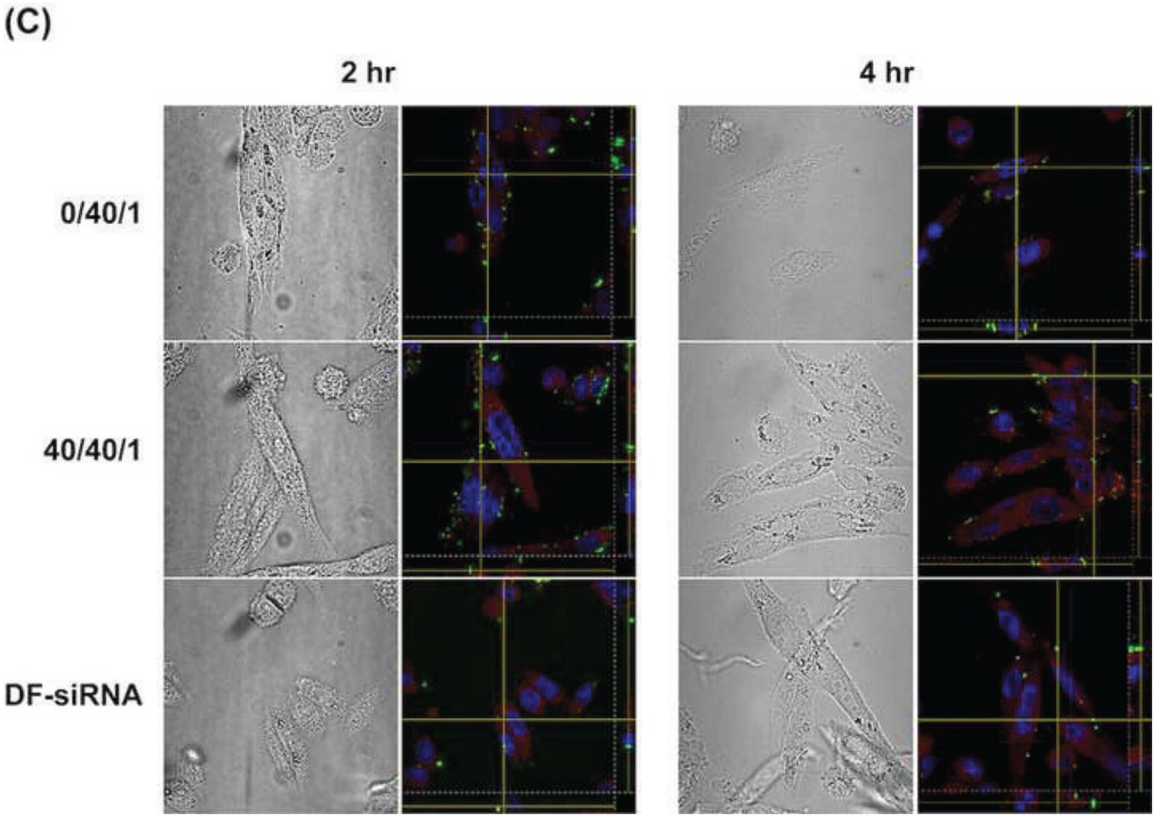


**Figure 6.**

Cellular uptake of Chi/FAM-siRNA (N/P ratio: 40/1) (A) and HA-coated Chi/FAM-siRNA (C/N/P ratio: 40/40/1) (B) complexes (magnification: 100X) in MP-38 cells under hypoxia conditions at different duration (1, 2, and 4 hr). (C) Z-stack images of cellular uptake of Chi/FAM-siRNA (N/P: 40/1) and HA-coated Chi/FAM-siRNA (C/N/P: 40/40/1) in MP-38 cells under hypoxia conditions at 2 hr and 4 hr, respectively. Images were taken by CLMS. Green signal: FAM; Blue signal: Hoechst; Red signal: LysoTracker™.

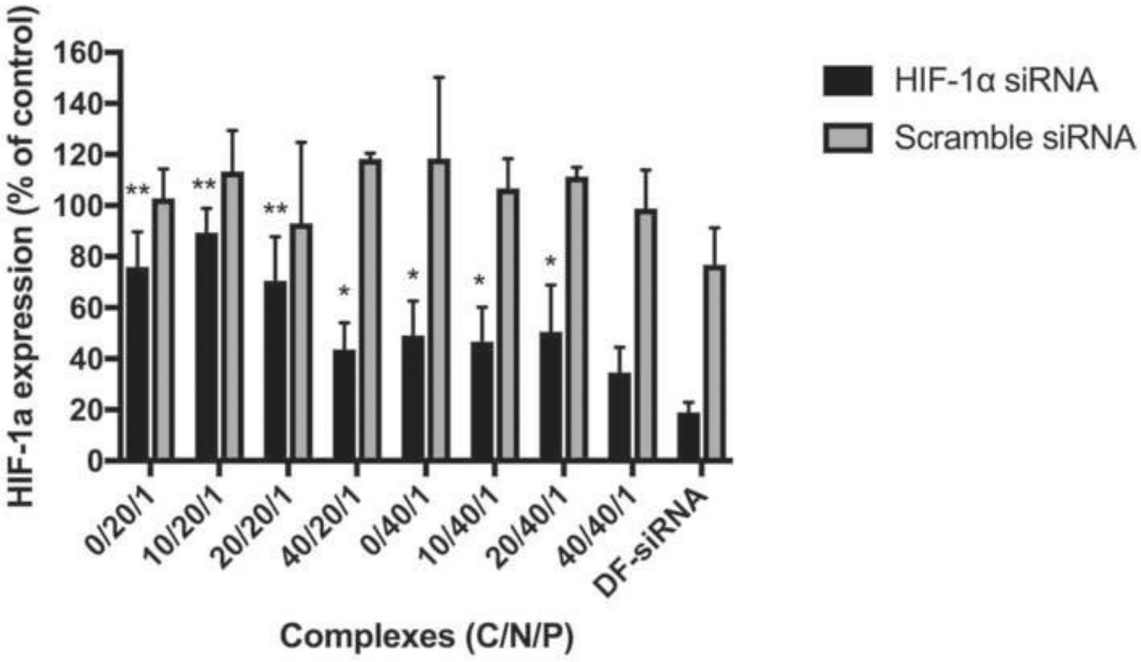


**Figure 7.**

HIF-1α mRNA expression level in MP-38 cells treated with siRNA complexes for 48 hr under hypoxia conditions. Statistical analysis comparing HIF-1α siRNA loaded complexes (with or without HA coating) with the DF-HIF-1α siRNA composite. *$p<0.05$; **$p<0.01$.

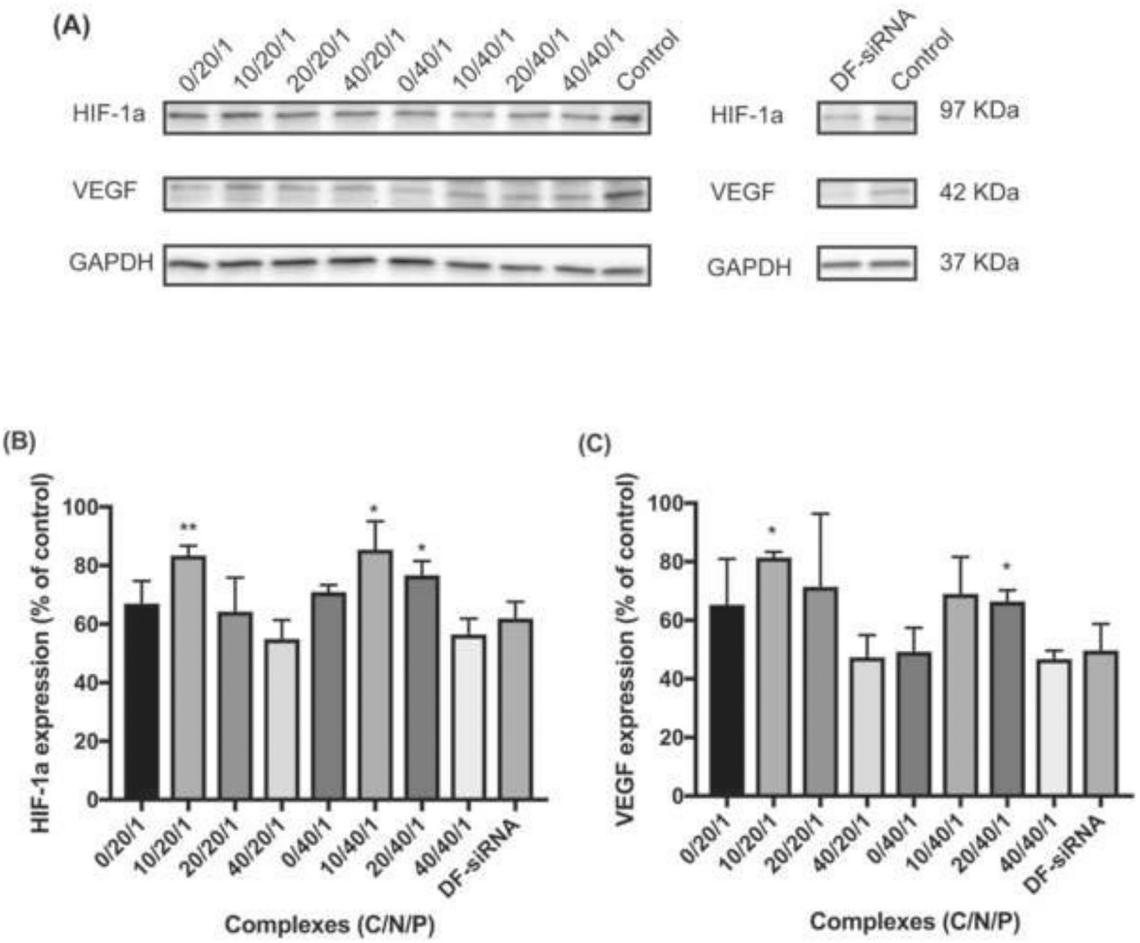


**Figure 8.**

Expression of HIF-1α and VEGF proteins in MP-38 cells after the treatment with Chi/siRNA complexes and DF-siRNA (A) under hypoxia conditions. Semi-quantification results of HIF-1α (B) and VEGF (C) protein expression in MP-38 cells after treated with the siRNA complexes. MP-38 cells without any treatment and grown under hypoxia conditions were used as a control. Statistical analysis comparing HIF-1α siRNA loaded complexes (with or without HA coating) with DF-HIF-1α siRNA composite. *$p<0.05$; **$p<0.01$. GAPDH housekeeping gene was used as an internal control in the quantification of target gene expression.

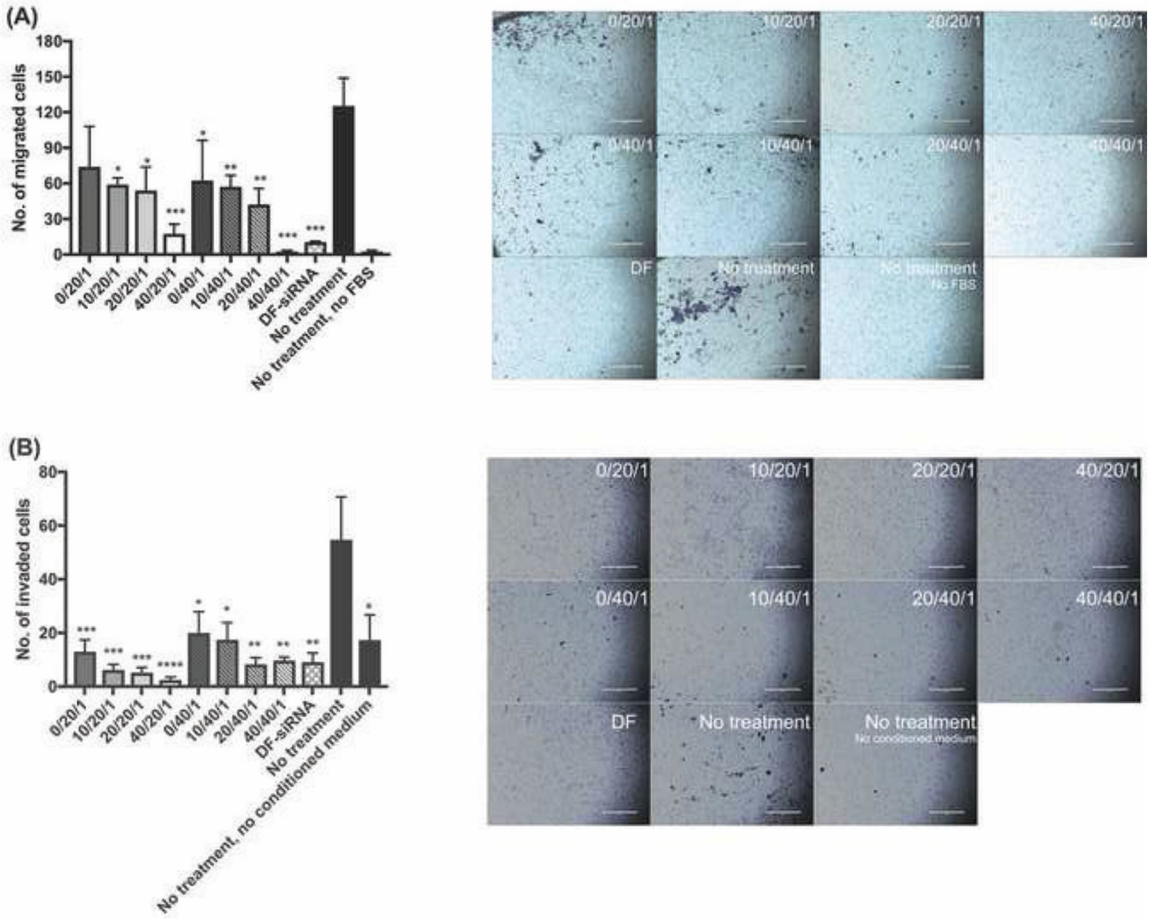


**Figure 9.**

(A) Migration and (B) invasion results of MP-38 cells following the treatment of siRNA complexes under hypoxia conditions. FBS and conditioned medium (DMEM containing 10% FBS used to culture NIH3T3 fibroblast cells) were used as a chemoattractant for migration and invasion studies, respectively. Statistical analysis comparing the complex-treated and control groups. *$p$<0.05; **$p$<0.01; ***$p$<0.001; ***$p$<0.0001, scale bar=400 μm. The different background color in the images was due to the presence of Matrigel coating.

**Table 1.**

Physicochemical characteristics of the prepared Chi/siRNA complexes.

| C/N/P (molar ratio) | Ave $D_H$ (nm) | Ave PDI | Ave $\zeta$ (mV) | siRNA loading efficiency (%) |
|---|---|---|---|---|
| 0/20/1 | 195.6 ± 2.55 | 0.38 ± 0.023 | 13.3 ± 2.00 | 83.53 ± 1.85 |
| 10/20/1 | 165.8 ± 2.80*** | 0.24 ± 0.011 | −18.0 ± 0.40 | 81.81 ± 1.70 |
| 20/20/1 | 169.3 ± 4.42*** | 0.29 ± 0.033 | −20.5 ± 0.99 | 83.34 ± 1.29 |
| 40/20/1 | 169.4 ± 5.39** | 0.19 ± 0.015 | −21.7 ± 3.43 | 83.50 ± 1.37 |
| 0/40/1 | 174.3 ± 7.72 | 0.26 ± 0.013 | 13.9 ± 1.44 | 89.15 ± 1.35 |
| 10/40/1 | 186.4 ± 5.66 | 0.19 ± 0.015 | −16.4 ± 0.15 | 91.75 ± 0.95 |
| 20/40/1 | 184.6 ± 13.1 | 0.28 ± 0.015 | −18.8 ± 0.21 | 90.02 ± 1.15 |
| 40/40/1 | 189.6 ± 3.71 | 0.16 ± 0.011 | −24.3 ± 1.06 | 88.98 ± 1.24 |
| DF-siRNA | 192.0 ± 7.42 | 0.31 ± 0.042 | 48.6 ± 3.53 | 89.69 ± 1.06 |

Statistical analysis comparing HA coated Chi/siRNA complexes to the non-coated Chi/siRNA complexes.

** $p<0.01$;

*** $p<0.001$.